The Journal of Experimental Biology 215, 2262-2272

doi:10.1242/jeb.070516

RESEARCH ARTICLE

Flexibility in starting posture drives flexibility in kinematic behavior of the kinethmoid-mediated premaxillary protrusion mechanism in a cyprinid fish, *Cyprinus carpio*

Nicholas J. Gidmark[1,*], Katie Lynn Staab[2], Elizabeth L. Brainerd[1] and L. Patricia Hernandez[2]

[1]Department of Ecology and Evolutionary Biology, Brown University, Providence, RI 02912, USA and [2]Department of Biological Sciences, The George Washington University, Washington, DC, USA

*Author for correspondence (nicholas_gidmark@brown.edu)

SUMMARY

Premaxillary protrusion in cypriniform fishes involves rotation of the kinethmoid, an unpaired skeletal element in the dorsal midline of the rostrum. No muscles insert directly onto the kinethmoid, so its rotation must be caused by the movement of other bones. In turn, the kinethmoid is thought to push on the ascending processes of the premaxillae, effecting protrusion. To determine the causes and effects of kinethmoid motion, we used XROMM (x-ray reconstruction of moving morphology) to measure the kinematics of cranial bones in common carp, *Cyprinus carpio*. Mean kinethmoid rotation was 83 deg during premaxillary protrusion (18 events in 3 individuals). The kinethmoid rotates in a coordinated way with ventral translation of the maxillary bridge, and this ventral translation is likely driven primarily by the A1β muscle. Analyses of flexibility (variability between behaviors) and coordination (correlation between bones within a behavior) indicate that motion of the maxillary bridge, not the lower jaw, drives premaxillary protrusion. Thus, upper jaw protrusion is decoupled from lower jaw depression, allowing for two separate modes of protrusion, open mouth and closed mouth. These behaviors serve different functions: to procure food and to sort food, respectively. Variation in starting posture of the maxilla alone dictates which type of protrusion is performed; downstream motions are invariant. For closed mouth protrusion, a ventrally displaced maxillary starting posture causes kinethmoid rotation to produce more ventrally directed premaxillary protrusion. This flexibility, bestowed by the kinethmoid–maxillary bridge–A1β mechanism, one of several evolutionary novelties in the cypriniform feeding mechanism, may have contributed to the impressive trophic diversity that characterizes this speciose lineage.

Key words: XROMM, jaw, biomechanics, stereotypy, flexibility, coordination.

Received 23 January 2012; Accepted 17 March 2012

INTRODUCTION

Upper jaw protrusion contributes to food acquisition in many groups of fishes, as well as to food processing in some groups (Motta, 1984; Drucker and Jensen, 1991; Hernandez et al., 2007). In most teleosts, jaw protrusion is characterized by significant correlation, i.e. obligate mechanical coupling, between lower jaw depression and upper jaw movements [‘mandible depression model’ (Motta, 1984)]. Recent work suggests that protrusion in cypriniform fishes involves decoupled movements of the upper and lower jaws (Staab et al., 2012). Cypriniform fishes (minnows, carps and their allies) protrude their premaxillae in two different ways (Fig. 1): open mouth protrusions, in which the mouth opens maximally in concert with buccal expansion during food gathering, and closed mouth protrusions, in which the mouth is minimally opened in concert with buccal expansion and the premaxilla is protruded in a more ventral orientation, during food processing (Sibbing, 1982; Sibbing, 1989). In this study, we focused on the precise mechanics of these two types of jaw protrusion in common carp (*Cyprinus carpio* Linnaeus).

Because common carp feed on decaying organic material on the bottom of streams and lakes (Sibbing, 1982), their feeding cycle is characterized by both suction feeding to acquire food items and intraoral processing of detritus. Open mouth protrusions are employed during suction feeding in synchrony with buccal expansion, resulting in a rapid flow of water through the mouth and into the buccal cavity (Fig. 1B). Along with this water comes a variety of food items, as well as unwanted items (sand, mud, etc.) of little or no food value. With this slurry in the buccal cavity, common carp use their muscular palatal organ to select food particles for ingestion (Sibbing, 1985). To sort this material and wash away the unwanted particles, the fish must move water both anteriorly and posteriorly in the buccal cavity. Water can be forced anteriorly in the buccal cavity by closing the mouth and protruding the upper jaws (Fig. 1C) (Drucker and Jensen, 1991; Callan and Sanderson, 2003). When the jaws are subsequently retracted, water is again flushed posteriorly. Subsequent cycling of protrusion and retraction with the mouth closed sorts food particles from non-food particles with the aid of the muscular palatal organ (Sibbing, 1985), and non-food particles are washed out through either the oral or the pharyngeal opening.

Upper jaw protrusion in common carp involves a novel skeletal element, the kinethmoid (kinetic ethmoid) (Fig. 2). The kinethmoid is a cypriniform synapomorphy and is ubiquitous across this clade of nearly 3500 species (Simons and Gidmark, 2010), with the exception of one highly miniaturized species (Britz et al., 2009). The kinethmoid is an unpaired, midline sesamoid bone or cartilage that develops within the intermaxillary ligament (Staab and Hernandez, 2010). In adult fishes it is suspended within a ligamentous network, with connections to the premaxillae, maxillae,

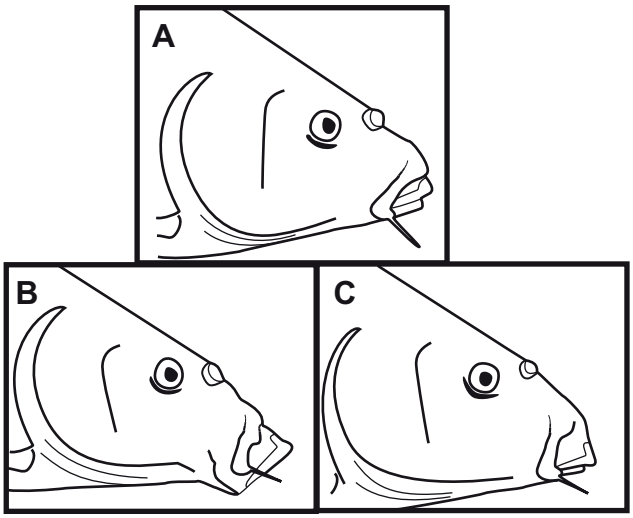

Fig. 1. Protrusion behaviors in common carp, *Cyprinus carpio*. (A) Resting state. (B) Open mouth protrusion. (C) Closed mouth protrusion. External, lateral views.

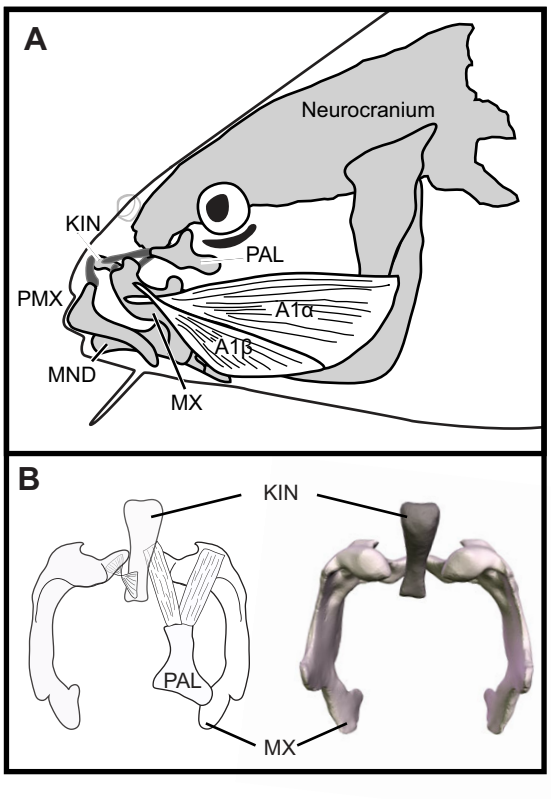

Fig. 2. Oral jaw anatomy in common carp. (A) Left lateral view. Ligaments are shown in dark gray, bones in light gray. Sections of the A1 muscle and their insertions are shown in white and overlaid on the bones. (B) Dorso-caudal view of maxillae (light gray) and kinethmoid (dark gray); drawing (left) and rendering (right). Ligamentous connections and approximate position of the palatine bone are included in the drawing. KIN, kinethmoid; PAL, palatine; PMX, premaxilla; MND, mandible, MX, maxilla.

palatines and neurocranium (Fig. 2). Maxillary connections to the kinethmoid originate on processes that we will refer to collectively as the 'maxillary bridge' ['median processes' (Alexander, 1966)]. The bridge is made up of these two bony median processes, one from each (left and right) maxilla that abut one another and unite the maxillae just anterior to the kinethmoid. During feeding, the premaxillae protrude and the distal end of the kinethmoid rotates forward toward the premaxillae, although the full extent of kinethmoid motion has never been quantified.

Despite many decades of study, the role of the kinethmoid in cypriniform premaxillary protrusion remains unclear (Hernandez et al., 2007). Some authors have postulated that the kinethmoid does not play an active role in protrusion, and instead the maxillae push directly on the premaxillae (Eaton, 1935), causing them to protrude (as is the case in perciform fishes). Others have postulated that the kinethmoid is pulled into rotation by the maxillae to push on the premaxillae (Giris, 1952; Alexander, 1966). Most recent evidence supports the latter hypothesis: maxillary movement causes kinethmoid movement, which then causes premaxillary movement (Ballintijn et al., 1972; Motta, 1984). In addition, the causes of maxillary motion are unclear. Alternative hypotheses of maxillary motion being caused by either a specialized division of jaw adductor musculature (A1β, Fig. 2A) or by lower jaw depression (*via* ligamentous connections between the upper and lower jaws) have been proposed (Alexander, 1966; Ballintijn et al., 1972).

Further complicating this debate, the fundamental mechanics of premaxillary protrusion might vary between open and closed mouth protrusions, as the bones are in a different configuration during each type of protrusion (Ballintijn et al., 1972). The position and orientation of one bone relative to another, i.e. bone posture, will dictate the mechanics (moment arms of ligaments, muscle lines of action, length–tension physiology of muscle, etc.) of any biomechanical system (German et al., 2011). Animators often use the term 'pose' to indicate the position and orientation of a rigid body; the biological literature uses the term 'posture' to encompass pose and include anatomical relationships as well. Understanding the dynamics (or maintenance) of one bone's posture relative to that of other bones throughout both protrusion behaviors could give insight into both the mechanics of the protrusion mechanism itself and ways in which it can be modulated to perform distinct behaviors.

Here, we used XROMM (x-ray reconstruction of moving morphology), an *in vivo* skeletal imaging technique, to reconstruct three-dimensional (3D) bone movements during open and closed mouth premaxillary protrusion in common carp, *C. carpio*. We tracked movement patterns of the neurocranium, premaxilla, maxilla, kinethmoid and mandible. By employing explicit anatomical coordinate systems to test mechanical hypotheses, we aimed to create a general model for kinethmoid-mediated premaxillary protrusion and outline a framework for future comparative work on the evolution of jaw mechanics in this group.

Specifically, we quantified coordination (congruent movement patterns of separate bones within a single behavior) (*sensu* Wainwright et al., 2008) to test the hypothesis that kinethmoid rotation causes premaxillary protrusion. We quantified flexibility (disparate movement patterns of a single bone during distinct behaviors) (*sensu* Wainwright et al., 2008) to test the hypothesis that the mechanism of premaxillary protrusion is independent of lower jaw depression. Finally, we quantified stereotypy (variation within behaviors) (*sensu* Wainwright et al., 2008) to test the hypothesis that bone movements during closed mouth protrusion behaviors are more consistent than those of open mouth protrusion behaviors. Ultimately, we used our kinematic data as a step towards understanding the protrusion mechanism by identifying potential mechanisms that our data do not support. We propose that, for a

hypothesis of causal relationship to be supported, two bone movements must be both highly coordinated and similar in their flexibility.

MATERIALS AND METHODS

Specimens

Three wild-type adult (300–400 mm) common carp, *C. carpio*, were obtained from farm-raised stock. We housed the fish individually in acrylic aquaria, each custom-built with a narrow extension (75–100 mm wide, ~300 mm long and the same height as the aquarium, 300 mm) that minimized the amount of water through which the x-ray beams must travel. The fish were allowed to swim into and out of the tunnel at will, but were trained to feed only at the end of the tunnel. All animal housing and experimental procedures were approved by Brown University's Institutional Animal Care and Use Committee.

Surgical and experimental protocols

Animals were anesthetized in a solution of bicarbonate-buffered MS-222 (Argent Chemical Laboratories, Redmond, WA, USA) for surgery. The initial concentration of 0.1 g l^{-1} was dropped to 0.075 g l^{-1} for maintenance during surgery. A rostral incision allowed access to deep portions of the maxilla and kinethmoid, while other bones were sufficiently superficial that skin incisions were unnecessary. A minimum of three tantalum metal spheres (0.5–0.8 mm in diameter) were implanted in each of the five bones of interest (kinethmoid, maxilla, premaxilla, mandible and neurocranium), for a minimum of 15 spheres (Fig. 3). In some cases, four markers in the neurocranium were implanted. The paired bones (mandible, premaxilla and maxilla) were marked unilaterally. Approximately 1 mm deep holes were drilled into the bones (0.8 mm manual drill bit, McMaster-Carr, Santa Fe Springs, CA, USA), and spheres were individually pressed into each hole. Marked bone regions were selected on the basis that the region was thick enough to support drilling and that markers were placed as far apart as possible in the bone for increased accuracy of movement reconstruction (Brainerd et al., 2010). Static x-ray pictures using a Faxitron cabinet x-ray machine (Hewlett-Packard, Palo Alto, CA, USA) and Polaroid film (Polaroid, Minnetonka, MN, USA) verified marker placement.

The fish were allowed to recover post-operatively until the surgical incisions had healed and normal feeding behavior had resumed. A biplanar x-ray video system constructed out of refurbished C-arm fluoroscopes (Radiological Imaging Systems, Hamburg, PA, USA) with 30 cm image intensifiers allowed us to capture marker movement over time. High-speed Photron (San Diego, CA, USA) 1024 PCI digital video cameras, mounted onto the fluoroscopes with custom-machined camera mounts, were used to record videos from the fluoroscopes at 125 frames s^{-1}, 80–120 kV and 4–20 mA.

Undistortion, calibration, digitizing and precision

We used the XrayProject workflow (Brainerd et al., 2010) to process the x-ray videos and reconstruct 3D movement data; we used XrayProject version 2.1.4 and earlier versions throughout this study. This set of Matlab scripts for XROMM analysis is freely available (and its implementation described in detail) at www.xromm.org. We will briefly describe its functionality here.

To remove distortion introduced by the image intensifiers, we imaged a precision-punched metal sheet. A distortion correction algorithm compared the spacing between the holes in the image with the standard spacing. To calibrate camera placement for each filming day, images were taken of a 32- or 64-point calibration cube constructed out of acrylic sheet and metal spheres at known distances. In each camera view, we tracked the (x, y) pixel positions of each bone marker over time. When videos were clear enough and marker overlap was minimal, the XrayProject tracking algorithm and centroid finder automatically tracked marker coordinates. When this was not the case, we tracked coordinates manually. To assess the precision of this method, we examined the standard deviation of the distance between rigidly attached marker pairs, i.e. markers within the same bone (Tashman and Anderst, 2003; Brainerd et al., 2010). Collating inter-marker distance standard deviations for 15 marker pairs per trial, 6 trials per individual and 3 individuals, our mean precision was ±0.0406 mm (N=270 pairwise inter-marker distances).

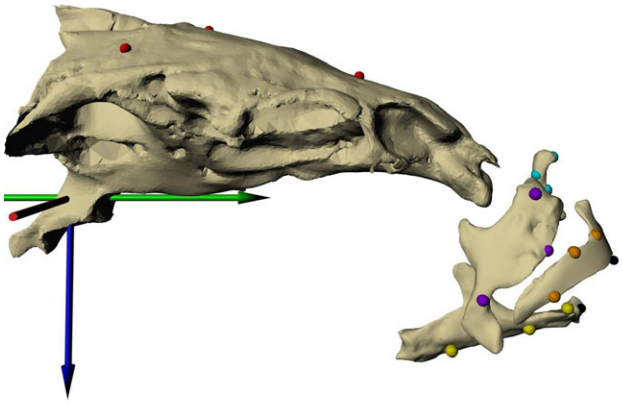

Fig. 3. Tantalum marker bead placement and anatomical coordinate system (ACS) in a representative individual (right lateral view). Marker placement for each individual fish was slightly different, but the markers were always placed as far apart as possible within each bone. The positions of the same markers within each bone of each individual were then determined and combined with *in vivo* marker movements to produce XROMM (x-ray reconstruction of moving morphology) animations. Neurocranium markers are shown in red; maxilla markers, purple; kinethmoid markers, cyan; premaxilla markers, orange; mandibular markers, yellow. Anatomical axis system, which is rigidly attached to the skull, shows vectors of ventral translation (z, blue), anterior translation (y, green) and lateral translation (x, red). Polarity of arrow indicates positive direction (red arrowhead is hidden behind neurocranium). Virtual markers (shown in black) were placed on the rostral tips of the premaxillae and mandible (and also on the maxillary bridge, not shown). These virtual markers move with the bones of interest and their positions were measured using the ACS.

Bone models, rigid body motion and XROMM animation

We used laser scans to digitally define the surface morphology of cleaned, dried bones and to generate 3D renderings of the bones for subsequent animation. Because the tantalum beads produce a scatter effect on CT scans, laser scanning is ideal for creating 3D surface models of small bones like those in the carp jaw. After cleaning the bones by dissection and dermestid beetles, we spray painted them with Rust-Oleum flat spray paint (Painter's Touch, Pleasant Prairie, WI, USA) and used a Microscan Tools scanner head with a Microscribe articulated arm (GoMeasure3D, Amherst, VA, USA) to generate models. We processed models in both Microscan Tools and GeoMagic (Research Triangle Park, NC, USA) software.

The XROMM workflow provides a method for calculating rigid body motion of any object from three or more points through

Table 1. Kinematic variables described relative to resting pose

Object	Data source[1]	Abbreviation	Description[2]
Maxillary bridge	ACS	BR_{tx}	Medial translation of the maxillary bridge
		BR_{ty}	Anterior translation of the maxillary bridge
		BR_{tz}	Ventral translation of the maxillary bridge
Tip of premaxilla	ACS	PMX_{tx}	Medial translation of the rostral tip of the premaxilla
		PMX_{ty}	Anterior translation of the rostral tip of the premaxilla
		PMX_{tz}	Ventral translation of the rostral tip of the premaxilla
Kinethmoid[3]	JCS	KIN_{tx}	Translation of the kinethmoid along its long axis
		KIN_{rx}	Rotation of the kinethmoid about its long axis
		KIN_{ty}	Anterior translation of the kinethmoid
		KIN_{ry}	Abduction of the distal end of the kinethmoid
		KIN_{tz}	Lateral translation of the kinethmoid
		KIN_{rz}	Rotation of the kinethmoid in the sagittal plane
Maxilla[3]	JCS	MX_{tx}	Anterior translation of the maxilla
		MX_{rx}	Abduction of the ventral arm of the maxilla
		MX_{ty}	Translation of the maxilla along its long axis
		MX_{ry}	Rotation of the maxilla about its long axis
		MX_{tz}	Lateral translation of the maxilla
		MX_{rz}	Rotation of the maxilla in a parasagittal plane
Mandible[3]	JCS	MND_{tx}	Dorsal translation of the mandible
		MND_{rx}	Rotation of the mandible about a dorso-ventral axis running through the quadrate–articular joint
		MND_{ty}	Anterior translation of the mandible
		MND_{ry}	Rotation of the mandible about a rostro-caudal axis running through the quadrate–articular joint
		MND_{tz}	Lateral translation of the mandible
		MND_{rz}	Jaw depression and elevation

[1]Type of axis system used to export data from XROMM animations: JCS (joint coordinate system) *versus* ACS (anatomical coordinate system).
[2]Polarity is determined by ACS orientation and right-hand rule; motion in the positive direction indicated here.
[3]These bone movements are relative to neutral bone positions at rest. As the bone moves, these coordinate systems move with the bone, thus shifting their orientations relative to the skull.

time by merging 3D bone models with 3D marker kinematics (Brainerd et al., 2010). To merge these two data streams, we took orthogonal images of cleaned bones using the biplanar fluoroscopy system, calibrated/undistorted as above, and imported these camera positions (and their respective images) into Autodesk Maya, a digital animation software package (Autodesk, San Rafael, CA, USA). We used Scientific Rotoscoping (Gatesy et al., 2010) to manually align bone models and marker models with both x-ray views to register marker placement with each bone. We calculated the rigid body transformations necessary to move markers from this reference pose to *in vivo* positions of one trial for each individual and applied the same transforms to the bone models for that individual.

Methods for movement description

We used two methods for describing movement in our XROMM animations: anatomical coordinate systems (ACSs) and joint coordinate systems (JCSs). ACSs provide an anatomically based frame of reference for describing the position (in x, y, z coordinates) of a point in space. We used these systems to track the movement of a specific point relative to, for example, the skull in separate, orthogonal directions (i.e. anterior, ventral and lateral directions). JCSs, in contrast, measure 6 degrees of freedom movements of one rigid body (e.g. a bone) relative to another. By employing both ACSs and JCSs, we gained a more complete understanding about what, for example, 30 deg of mandible depression (JCS, relative to the skull) means in terms of the distance traveled by the mandible tip (in the skull ACS frame of reference). We were also better able to understand the changes in gape that result from simultaneous mandibular depression and protrusion. These distinct coordinate systems are described separately below.

ACS and virtual marker placement

We placed an ACS, using a tool from the XROMM Maya Shelf, centered on the cranio-vertebral joint. This coordinate system is made up of three orthogonal axes and is rigidly attached to the skull. One advantage of this tool is that we can align this coordinate system with anatomically relevant landmarks, given our high-resolution bone models (Gatesy et al., 2010). We aligned the z-axis of the coordinate system with the sagittal crest at the back of the skull, at the site of epaxial musculature attachment, which we used to define the dorso-ventral axis of movement relative to the skull. We aligned the y-axis with the midline of the skull, using it to define the anterior–posterior axis of movement relative to the skull. The x-axis is perpendicular to the y- and z-axes, and is thus oriented medio-laterally.

We can attach virtual markers to points of interest on any animated bone and track the position of that marker in the ACS. We began by creating two virtual markers using Maya locators: one on the anterior tip of the premaxilla and one on the maxillary bridge (Table 1, Fig. 3). As the animal moves, the ACS measures movement of these landmarks relative to the skull. As the ACS gives xyz coordinates of these locators, we can independently record both the ventral (z-axis value) and anterior (y-axis value) positions, therefore teasing apart these components of the movement relative to the skull. In cases where distances instead of positions were important, such as in measuring gape and protrusion, we used a pair of virtual markers, exported their positions in the ACS, and calculated the 3D distance between the two points over time. This method allows typical measurements such as gape to be collected in much the same way as classical standard video data sets are collected: the distance between a point on the tip of the premaxilla and another on the tip of the mandible measures gape. As we were using 3D bone models,

we measured protrusion distance as the distance between the anterior tip of the premaxilla and the anterior tip of the neurocranium.

JCSs

For examining whole-bone kinematics, we used JCSs (Grood and Suntay, 1983; Gatesy et al., 2010; Brainerd et al., 2010; Dawson et al., 2011). A JCS is a hierarchical set of axes similar to an ACS, except that the association is between the 3D pose of two bones instead of a single bone and a point. Whereas in an ACS all three axes are attached to the bone of interest (in the case above, all are attached to the skull), in a JCS the highest order axis (in our case, the *z*-axis) is attached to a proximal bone, and the lowest order axis (in our case, the *x*-axis) is attached to the distal bone. The intermediate (*y*-axis) axis is calculated for each position and is perpendicular to the other two axes. By placing the proximal JCS in an anatomically explicit position, we can describe movement of a distal bone in a coordinate system defined by these axes and relative to a proximal bone's movement in all six degrees of freedom – translation along each of the three axes and (ordered) rotation about each of them.

Conventional JCS methods (Grood and Suntay, 1983) use the highest order axis (sometimes labeled *x*-axis, but labeled *z*-axis in the Maya XROMM tools) to describe the greatest amount of motion. For all three JCSs in the carp jaw, we aligned the *z*-axis medio-laterally to encompass as much movement as possible as *z*-axis rotation. For the kinethmoid, we positioned the origin of the axis system at the proximal base of the kinethmoid and aligned the *x*-axis with the long axis of the bone (Fig. 4A). We set the kinethmoid rotation about the *z*-axis (medio-lateral axis) such that the zero position corresponded to time points where the kinethmoid is directly vertical relative to the anterior–posterior axis of the fish. Positive rotations about this medio-lateral axis result in the dorsal end of the kinethmoid moving anteriorly (Fig. 4A).

For the maxilla, we fitted a sphere to the surface where it articulates with the second pre-ethmoid cartilage [see Conway et al. for a description of these cartilaginous elements (Conway et al., 2010)], positioned the origin of this axis system at the center of the sphere, and aligned the *y*-axis to the long axis of the bone (Fig. 4B). The long axis of the maxilla is not directly parallel to the dorso-ventral axis of the skull. Therefore, our maxillary *y*-axis maintains a deviation from vertical (approximately 10°), resulting from lateral abduction of the ventral end of the maxilla. This deviation also results in a measurement of rotation about the *z*-axis (rotation in the sagittal plane) that is not identical to the *z*-axis rotations of other bones in this study. For the mandible, we positioned the origin of the axis system at the center of the jaw joint. As we did not animate the quadrate, we used the articular bone's articular surface to define the radius of the jaw joint surface, positioning the axis system equidistant from all points on the articular surface (Fig. 4C). We created JCSs with animated bones from a single protrusion event. For consistency, we reused this same JCS placement in different trials of a given individual by reanimating the entire set of bones, with JCSs attached, using kinematic data from the other five trials for that individual. Within each individual, we created a JCS for the lower jaw, the kinethmoid and the maxilla. In each case, the proximal bone was the skull.

With six degrees of freedom per JCS (three rotations and three translations), and three joints each having their own coordinate system, a total of 18 degrees of freedom comprise our JCS dataset. To organize this dataset, we gave each axis system a set of letters to denote the distal bone: MND for the mandible, MX for the maxilla and KIN for the kinethmoid. We followed these bone letters with either 'r' or 't' (subscript), to denote either rotations about or translations along each axis. We then used '*x*', '*y*' or '*z*' to denote the specific axis. Therefore, KIN_{rz} would refer to kinethmoid rotation about the *z*-axis, MX_{ty} would refer to maxillary translation about the *y*-axis or long axis of the bone. Thus, for example, KIN_{rx} is always rotation about the long axis of the kinethmoid, and KIN_{tx} is always translation along the long axis. As the *x*-axis is attached to the kinethmoid while it undergoes rotation about the *z*-axis, KIN_{tx} would produce a dorsal translation of the kinethmoid when KIN_{rz}=0 deg, but a rostral translation when KIN_{rz}=90 deg. We summarize all 18 degrees of JCS freedom in Table 1.

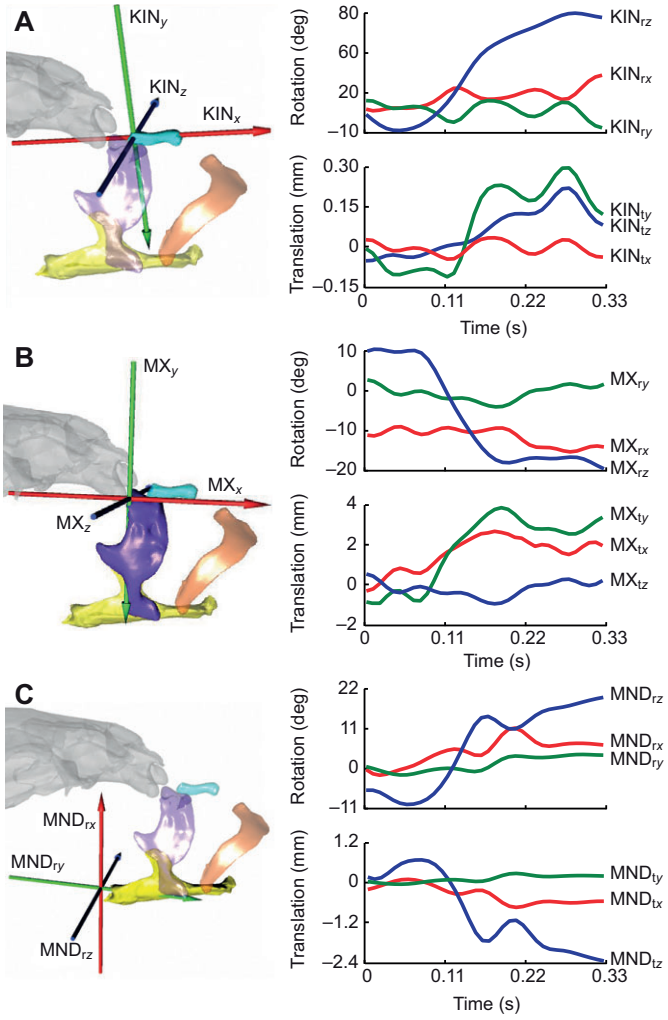

Fig. 4. Representative plots of 6 degrees of freedom bone motion data during an open mouth protrusion. (A) Kinethmoid; (B) maxilla; (C) mandible. Axis orientation determines the polarity of the readings by the right-hand rule, such that positive translation along the blue *z*-axis in A, for example, moves the kinethmoid toward the animal's left side, and positive rotation about that axis rotates the kinethmoid clockwise in this view. Note that in B, rotation of the maxilla about the medio-lateral *z*-axis decreases throughout the protrusion; whereas other bones rotate *via* the dorsal end moving anteriorly, the maxilla rotates with the ventral end moving anteriorly. *x*-axis is in red, *y*-axis in green; *z*-axis in blue.

Data analysis

As we were primarily interested in the effect of kinethmoid rotation for each trial, we examined time series data from the onset of

Table 2. Movement magnitudes and relative timing of variables

	Type	Gape	KIN_{rz}	PMX_{ty}	MND_{rz}	BR_{tz}	MX_{rz}	MX_{ty}	BR_{ty}	MX_{ry}
Magnitude[1]	Open	12.8±4.59	83.0±23.90	10.1±3.68	38.0±6.82	3.1±1.32	29.9±6.64	5.5±3.21	3.6±1.73	8.5±2.38
	Closed	2.4±0.75	65.9±13.97	8.6±1.87	20.1±3.63	1.3±0.44	8.2±1.67	4.8±1.73	2.8±0.86	7.2±0.72
Lag time[2]	Open	0.00±0.00	N/A	0.00±0.00	0.00±0.00	0.00±0.00	–0.011±0.0188	0.061±0.0213	–0.307±0.0588	–0.115±0.0898
	Closed	0.00±0.0026	N/A	0.00±0.00	0.00±0.00	0.00±0.00	–0.011±0.0351	0.061±0.0189	–0.307±0.0351	–0.115±0.00

[1]Mean (±s.e.m.) change within a protrusion event. Note that these are delta values, i.e. initial position subtracted from the final position. (Rotations are in deg, translations and distance measurements are in mm.)

[2]Mean (±s.e.m.) time shift of variable (in s), earlier (+) or later (–) than kinethmoid for maximum correlation.

For definition of abbreviations, see Table 1.

kinethmoid movement to maximum protrusion, plus an additional 15% of trial duration at the beginning and the end of the trial. We used this time window for every variable in any given trial; the extended time on either end of the protrusion sequence allows for more accurate performance of the correlation algorithm discussed below. We tested three main hypotheses in this study, and each hypothesis was tested using a different metric of variability.

To test whether kinethmoid rotation is correlated with premaxillary protrusion, we used the principle of coordination (*sensu* Wainwright et al., 2008), or similarity between movement patterns of distinct bones within a trial. To perform this test, we treated each variable (each bone's movement) as a wave through time (i.e. a kinematic plot of distance or degrees over time), measuring the correlation of one wave with another using a custom-written Matlab script. As we are examining the drivers and outcomes of kinethmoid rotation, we calculated correlation (covariance) coefficients of each movement relative to KIN_{rz} (kinethmoid sagittal rotation) using the Matlab command 'xcov'. The same command was also used to determine the effects of phase changes (lag times) of one wave relative to another on these coefficients. Values for the correlation can range between 1 (perfectly identical) and –1 (perfectly out of phase and complementary). Values at zero show no correlation between waveforms, signifying no relationship between two movements.

To test whether the mechanism of premaxillary protrusion is independent of lower jaw depression, we used the principle of flexibility (*sensu* Wainwright et al., 2008), or variation between open and closed mouth protrusion behaviors. We quantified flexibility by conducting a nested ANOVA (behavior nested within individual) to compare open and closed mouth protrusions.

To test our final hypothesis, that open mouth protrusion behaviors are more variable than closed mouth behaviors, we used the principle of stereotypy, or consistency between trials of a given behavior (*sensu* Wainwright et al., 2008). We quantified stereotypy by calculating the coefficient of variation in magnitude of each variable – dividing the standard deviation by the mean. By comparing the coefficient of variation of open mouth protrusion behaviors with that of closed mouth protrusion behaviors of each bone motion, we can identify which behavior is more stereotyped, i.e. which has a lower coefficient of variation.

RESULTS

When carp first approach food, they open their mouths and protrude the premaxillae. During this open mouth protrusion, XROMM animations showed substantial kinethmoid rotation in the sagittal plane (Fig. 4A). We quantified kinethmoid movement in all 6 degrees of freedom and found up to 127 deg of rotation in kinethmoid sagittal rotation (KIN_{rz}) during initial food gathering. In nine food-gathering events, mean KIN_{rz} was 83.0 deg; other rotations were smaller (<30 deg) and observed in some trials but not others. All translations of the kinethmoid were small (<0.5 mm) and inconsistent. Note that as the kinethmoid moves, the joint axis system moves with the bone (Fig. 4A).

Primary rotation of the maxilla during open mouth protrusions was in a roughly parasagittal plane (MX_{rz}), about the medio-lateral *z*-axis (Fig. 4B). The ventral end of the maxilla moved anteriorly while the dorsal articulation with the second pre-ethmoid cartilage remained relatively static. Mean MX_{rz} was 29.9 deg (Table 2). We observed little long axis rotation or lateral flaring of the maxilla.

Translation of the maxilla was dominated by translation along its long axis (MX_{ty}; Fig. 4B). We observed no consistent anterior or lateral translations. Mean MX_{ty} was 5.5 mm in open mouth protrusions (Table 2).

The primary rotational component of mandibular movement that we observed was mandible depression and elevation (rotation about MND_{rz}, Fig. 4C). Rotation was almost exclusively in this axis, with a mean of 38.0 deg for open mouth protrusions (Table 2). We observed only slight and inconsistent rotation about the anterior–posterior axis of the mandible (MND_{ry}). We did observe rotation about the dorso-ventral axis, MND_{rx} (Fig. 4C; red line in rotation plot). As the mandibular symphysis remains intact (i.e. the two dentaries remain articulated, but the symphysis is flexible) during protrusion, MND_{rx} movement must occur in synchrony with MND_{tz}; lateral flaring of the jaw joint requires both lateral translation of the jaw joint and rotation about the symphysis.

In our cross-correlation analysis, several of the variables were most strongly correlated with little or no phase shift relative to rotation of the kinethmoid. Gape distance, protrusion distance, mandible depression (MND_{rz}), ventral bridge translation (BR_{tz}) and maxillary *z*-rotation (MX_{rz}) were all consistently synchronous with rotation of the kinethmoid (Table 2). Anterior translation of the maxillary bridge (BR_{ty}) was consistently late in the sequence and was only weakly correlated with KIN_{rz}, suggesting a lack of coordination between these motions (Table 3). Long axis rotation of the maxilla (MX_{ry}) occurred after kinethmoid rotation, while translation along this same axis (MX_{ty}) occurred just before kinethmoid rotation. Possibly most influential on our kinematic model, MX_{ty} is optimally correlated with rotation of the kinethmoid if shifted earlier than KIN_{rz} (Table 2).

Kinematic correlation

A primary goal of this study was to test hypotheses for whether movements of the maxilla and lower jaw may contribute to rotation of the kinethmoid and ultimately premaxillary protrusion. Because coordination is defined as the relative timing of anatomical movements (*sensu* Wainwright et al., 2008), we contend that the shape of the kinematic waveform (e.g. protrusion distance as a function of time) provides more detailed information about how protrusion occurs than just start, end or maximum protrusion time. As such, we find it necessary, though not sufficient, that for a given

Table 3. Coordination, flexibility and stereotypy (*sensu* Wainwright et al., 2008) of skeletal movements in this study

	Type	Gape	KIN_{rz}	PMX_{ty}	MND_{rz}	BR_{tz}	MX_{rz}	MX_{ty}	BR_{ty}	MX_{ry}
Coordination[1]	Open	N/A	N/A	0.967	0.912	0.988	0.695	0.809	0.176	0.079
	Closed	N/A	N/A	0.949	0.915	0.989	0.876	0.835	0.311	0.309
Flexibility[2]	Open *versus* closed	0.002	0.091	0.249	<0.001	0.0746	<0.001	0.599	0.0397	0.170
Stereotypy[3]	Open	2.02	1.62	2.04	5.63	2.71	1.25	3.31	3.37	1.57
	Closed	0.47	1.19	1.23	1.02	1.74	1.15	2.02	1.96	0.56

[1]Average correlation coefficient of each motion as compared to KIN_{rz}, sagittal rotation of the kinethmoid.
[2]*P*-value of nested ANOVA comparing the magnitudes of motion between open and closed protrusions.
[3]Coefficient of variation, calculated as standard deviation divided by mean. Lower values indicate greater stereotypy.
For definition of abbreviations, see Table 1.

movement (represented by a wave form) to cause a second movement (represented by a second wave form), the first movement must be highly coordinated with the second. We calculated cross-correlation coefficients of each bone movement with KIN_{rz} and used those correlation coefficients as a proxy for coordination (Table 3).

Premaxillary protrusion (PMX_{ty}) is highly coordinated with KIN_{rz}: coefficients averaged 0.967 and 0.949 for open and closed protrusions, respectively (Table 3). The movement most highly coordinated with kinethmoid rotation in our dataset is maxillary bridge ventral translation (BR_{tz}, coefficients of 0.988 for open and 0.989 for closed mouth protrusions). Correlation coefficients for mandibular depression (MND_{rz}) are also high for both open and closed protrusions (0.912 and 0.915, respectively), as are correlations with maxillary parasagittal rotation (MX_{rz}) for both open and closed protrusions (0.695 and 0.876). The other variables we measured are not coordinated with kinethmoid rotation (Table 3). Correlations were typically higher in closed than in open mouth protrusions.

Open *versus* closed protrusion behaviors

Another hypothesis we are testing is the independence of the upper jaw protrusion mechanism from the lower jaw depression mechanism. By identifying which of those mechanisms is flexible *versus* inflexible between behaviors, we can further refine our mechanical hypotheses and identify the presence (or absence) of decoupling between these mechanisms. To accomplish this, we first differentiated open and closed mouth protrusion events using both observations of XROMM animations and kinematic plots. Open mouth protrusion events were usually the first of many protrusions during a single feeding event and were associated with a suction feeding strike in which prey was captured. We differentiated open *versus* closed mouth protrusions by the fact that the lower jaw was rotated (depressed) by either >30 deg in open mouth protrusions or <25 deg in closed mouth protrusions. This also corresponded to a gape distance of >8 mm in open mouth protrusions and a gape distance of <5 mm in closed mouth protrusions (Figs 5, 6; Table 2). Because our measurement of gape was made using locators on the bones, this metric does not account for actual closure of the fleshy lips; therefore, gape was never zero even when the mouth was fully closed. While the gape remained near zero in closed mouth protrusions, the kinethmoid rocked back and forth, contributing to the increase and decrease in buccal volume during food processing (Fig. 5B).

Surprisingly, most movements that we investigated (premaxillary protrusion distance, KIN_{rz}, MX_{ty}, MX_{ry}, BR_{tz} and BR_{ty}) did not differ in magnitude between open and closed mouth protrusions (Table 3, Fig. 5). The main statistically significant differences that we observed (aside from a smaller gape) were decreases in MX_{rz} and MND_{rz} (Tables 2, 3).

We observed differences in the starting posture (i.e. relative position and orientation) of key structures between open and closed mouth protrusions. Whereas gape, for example, begins with the same value in open and closed protrusions and simply does not increase as much (i.e. does not show as high a magnitude of movement) in closed mouth protrusions, the maxillary bridge is in a different posture at the beginning of closed *versus* open mouth protrusion events (Fig. 6). In open mouth protrusions, the bridge starts at a position 7 mm ventral to the defined anterior–posterior axis of the skull, while during closed mouth protrusions, the sequence begins with a more ventral posture – 12 mm ventral in the same coordinate system. Regressions of this bridge translation with kinethmoid rotation show identical slopes between protrusion behaviors but significantly different intercepts (Fig. 7A,B). A similar pattern is observed in the position of the anterior tip of the premaxilla in the same coordinate system: the premaxilla begins the protrusion event

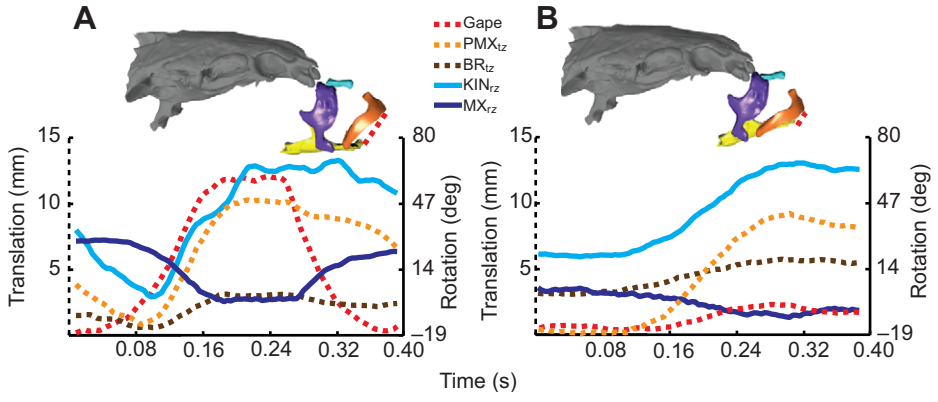

Fig. 5. Behavioral flexibility in the protrusion mechanism. Point-based distance measurements (dashed lines in warm colors, left *y*-axis) and whole-bone kinematics (solid lines in cool colors, right *y*-axis) during an open mouth protrusion (A) and a closed mouth protrusion (B). An example of a point-based measurement (gape) is shown in the rendering. Note similar patterns in kinethmoid rotation (KIN_{rz}, cyan), protrusion (orange) and bridge translation (brown) and different patterns in maxilla sagittal rotation (MX_{rz}, dark blue) and gape (red).

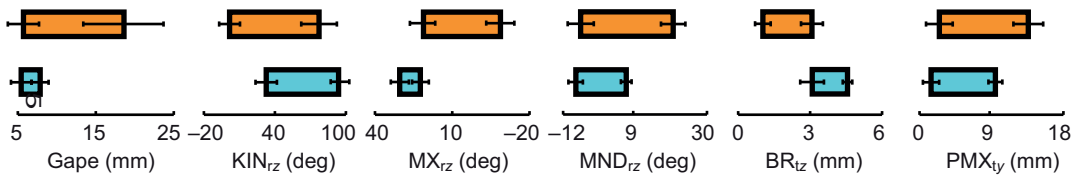

Fig. 6. Movements in open (orange) and closed (cyan) mouth protrusions. Each movement begins at the left end of the graph and proceeds to the right. Error bars denote s.e.m. of the posture at the beginning (left) and end (right) of protrusion. No aspect of timing is presented here, only the starting and ending value, i.e. the range of postures used during a given protrusion. Note that MX$_{rz}$ has a movement orientation opposite to that of the other bones, so we have inverted the polarity of the *x*-axis here, for clarity. Note how gape begins at the same position (~6 mm) but ends at either 18 mm (open mouth protrusions) or 8 mm (closed mouth protrusions), whereas MX$_{rz}$ and BR$_{tz}$ start and end at different absolute positions. In general, note that open mouth protrusions utilize a greater range of motion, though this is not always statistically significant.

in a more ventral posture during closed mouth protrusions, despite a similar amount of ventral translation throughout the behavior (Fig. 7C,D).

Kinematic consistency

Our final statistical comparison tested the relative stereotypy of both open and closed mouth protrusion behaviors. In every skeletal motion that we measured, we observed more stereotypy (a lower coefficient of variation) during closed mouth protrusions than during open mouth protrusions (Table 3). Some variables, such as MX$_{ry}$, were more stereotyped across behaviors than other variables, such as MX$_{ty}$, but overall, greater variation was typically observed in open *versus* closed mouth protrusions.

DISCUSSION

Kinethmoid rotation during premaxillary protrusion in cypriniforms has been suggested by several studies (Alexander, 1966; Ballintijn et al., 1972; Motta, 1984; Hernandez et al., 2007; Danos and Staab, 2010), but never before observed directly in living fish. Here, we used XROMM to visualize and measure kinethmoid motion and to demonstrate the importance of specific maxillary movements in eliciting rotation of the kinethmoid. We have also shown how careful examination of specific types of kinematic variation during premaxillary protrusion offers insights into both the fundamental protrusion mechanism and the specific mechanisms of closed and open mouthed protrusion. These findings underscore the importance of posture (relative position, orientation and mechanical connections between bones) in functional studies.

Our results support the hypothesis that kinethmoid rotation directly causes premaxillary protrusion in common carp. Rotation of the kinethmoid moves its dorsal end rostrally, and it pushes *via* a ligament on the premaxilla, causing protrusion; the same result can be accomplished *via* manual manipulation of anesthetized or freshly killed animals. The ligamentous attachment between these bones is histologically suited to act in compression, as it is enriched with hyaline cell cartilage and low in fibrous tissue (Benjamin, 1989), and the ontogenetic onset of protrusion coincides with kinethmoid ossification (Staab and Hernandez, 2010). We have not attempted to investigate the forces imposed *in vivo* on the premaxilla by protrusion or tested the material properties of this ligament, though this could be a fruitful approach. In this study, we were most focused on the drivers of kinethmoid rotation, and we describe our mechanical model below.

The ligamentous connection between the mandible and the maxilla necessarily couples their movements, with mandibular depression causing sagittal rotation of the maxilla about the point of its articulation with the second pre-ethmoid cartilage. As mandibular depression (MND$_{rz}$) and sagittal rotation of the maxilla (MX$_{rz}$) vary substantially in magnitude between open and closed mouth protrusions, whereas kinethmoid rotation (KIN$_{rz}$) does not, we reject those movements as primary drivers (either direct or indirect) of kinethmoid rotation (Table 2, Fig. 6). Given the lack of coordination (Table 3) between kinethmoid rotation and rostral bridge translation (BR$_{ty}$) or long axis rotation of the maxilla (MX$_{ry}$), we also reject those movements as primary drivers of kinethmoid rotation.

The inflexibility in kinethmoid rotation and MX$_{ty}$ (long axis translation of the maxilla) and their strong correlation (correlation coefficient of 0.809 and 0.835 with kinethmoid rotation, Table 3) suggest that MX$_{ty}$ is driving kinethmoid rotation in both open mouth and closed mouth protrusions. The high correlation of BR$_{tz}$ (ventral maxillary bridge translation) with kinethmoid rotation (0.988) indicates that this aspect of maxillary movement is most important for kinethmoid rotation. We hypothesize that MX$_{ty}$, perhaps in concert with other slight movements (such as MX$_{ry}$) that were below our resolution threshold, cause the maxillary bridge to translate ventrally (BR$_{tz}$), thus effecting kinethmoid rotation and leading to premaxillary protrusion.

Hence, ventral bridge translation appears to be caused primarily by ventral maxillary translation, but what causes the maxilla to slide ventrally? We propose that, as the A1β muscle fires (see Osse et al., 1997), its ventro-posterior line of action is opposed only by the second pre-ethmoid cartilage, which restricts maxillary movement into a primarily ventral direction. During open mouth protrusion events, this movement occurs in concert with mandibular depression, and thus the maxilla also rotates parasagittally (MX$_{rz}$). However, as A1β inserts on the maxilla, there is potential for ventral translation of the maxilla without sagittal rotation. The action of A1β alone, we propose, is capable of producing complex maxillary movement, dominated by MX$_{ty}$ (and bolstered by other, smaller motions), causing the kinethmoid to rotate.

Ballintijn and colleagues suggested that the fundamental mechanics of this protrusion can be changed during open and closed mouth protrusions, because the mandible is in a different starting/initial configuration (Ballintijn et al., 1972). Electromyographic data from that study indicate that if the animal has a completely closed mouth, the A1β muscle is not capable of premaxillary protrusion, serving instead to close the mouth and retract the premaxilla. Motta infers from these data that protrusion through A1β contraction is not possible (Motta, 1984). However, as long as the lower jaw is at least minimally depressed (as is the case during all of the trials we investigated of both open and closed mouth protrusions), the line of action of this muscle is fully capable of causing protrusion [as supported by previous studies (Alexander, 1966; Ballintijn et al., 1972; Osse et al., 1997)]. Furthermore, our data show nearly twice as much mandibular depression in open

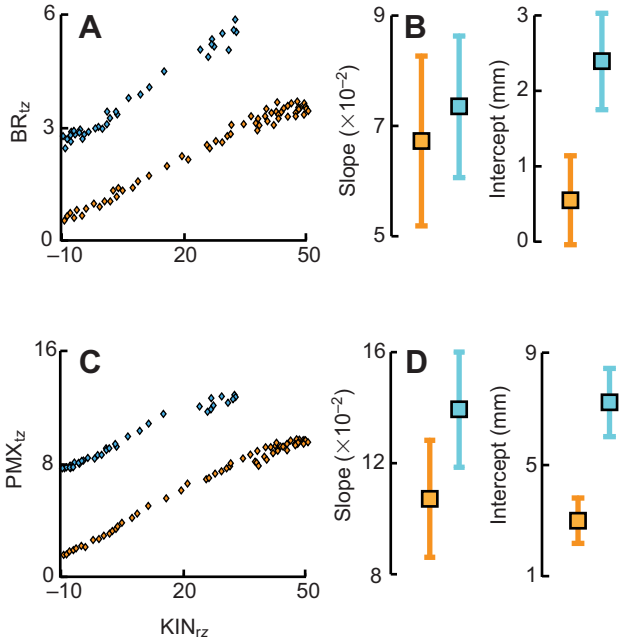

Fig. 7. Bone posture in open (orange) and closed (cyan) mouth protrusions. Bridge location (A,B) and ventrally directed protrusion (C,D) with kinethmoid rotation. A and C show a single representative open mouth protrusion event in orange and a single representative closed mouth protrusion event in cyan. B and D show mean ± s.e.m. of slopes and intercepts of the regressions for all protrusion events (N=9 open mouth protrusion events and 9 closed mouth protrusion events). Intercepts correspond to the position of that parameter when the kinethmoid is in its 0 deg posture, or directly vertical. BR_{tz} is bridge translation in the ventral direction; KIN_{rz} is sagittal rotation of the kinethmoid; PMZ_{tz} is premaxilla translation in the ventral direction. See Table 1 for more detailed descriptions of these variables.

mouthed protrusions as in closed mouth protrusions. If mandibular depression were driving the system, maxillary movements would show the same flexibility; however, they are inflexible between behaviors. Therefore, we maintain that A1β is the primary driver of the maxillary movements leading to kinethmoid rotation and premaxillary protrusion in common carp.

Coordination: kinethmoid rotation causes premaxillary protrusion

We use coordination (correlation between bone movements) (*sensu* Wainwright et al., 2008) as an indication of possible mechanical coupling – a necessary condition, though not, on its own, fully sufficient to prove a mechanism. We propose that, for a hypothesis of causal relationship to be supported, two bone movements must be both highly coordinated and similar in their flexibility (see below for discussion of flexibility). Thus, our coordination analysis becomes the first step in defining a mechanism by providing a set of prospective mechanical hypotheses of how the kinethmoid is rotated. Protrusion distance is highly coordinated with KIN_{rz}, which supports the hypothesis that kinethmoid rotation causes premaxillary protrusion. The drivers of kinethmoid rotation, according to our coordination analysis, could be mandibular depression (MND_{rz}), or ventral translation of the maxillary bridge (BR_{tz}). Of these, BR_{tz} has the highest coordination value; we hypothesize that it is the proximate driver of kinethmoid rotation. However MND_{rz} could also be required for protrusion. To fully understand the roles of BR_{tz}, MX_{rz} and MND_{rz} in causing kinethmoid rotation, we must also examine flexibility in these variables between behavior types.

Flexibility: kinethmoid rotation is driven primarily by maxillary bridge translation

The presence of both open and closed mouth protrusions indicates flexibility (variability between behaviors) (*sensu* Wainwright et al., 2008) in some aspect of the protrusion mechanism. By exploring which cranial movements show little flexibility between behaviors, we gained insight into which variables are key aspects of protrusion. The magnitudes of KIN_{rz}, BR_{tz} and protrusion distance are inflexible between behaviors: they are similar whether the animal is performing an open mouth protrusion or a closed mouth protrusion (Table 3). In contrast, other variables do show flexibility; for example, the starting posture of the maxilla (as demonstrated by the starting position of the bridge, BR_{tz}) is different in these two protrusion behaviors (Fig. 6). By starting the protrusion behavior with a slightly more ventrally positioned maxillary bridge, the protrusion mechanism can be modulated to perform a closed mouth protrusion as opposed to an open mouth protrusion. Importantly, this different starting posture need not dictate a change in mechanics; the slope of the regression between kinethmoid rotation and bridge translation (Fig. 7) is similar (i.e. inflexible) between behaviors – only the intercept is different (i.e. flexible). Inflexible slopes of these regressions indicate that a similar amount of kinethmoid rotation is obtained with a given amount of bridge translation. The distinct flexibility in intercept (i.e. the position of the maxillary bridge when the kinethmoid is directly vertical) indicates that the bridge is more ventral during a closed mouth protrusion (Fig. 7B). We observed the same pattern in the ventral component of premaxillary protrusion (Fig. 7C,D). Thus, we hypothesize that, by positioning the bridge more ventrally, the protrusion mechanism itself can be conserved between these behaviors but also modulated to deflect the premaxilla more ventrally (Fig. 1C). This ventral orientation of premaxillary protrusion, coupled with a lower magnitude of rotation in MND_{rz} (mandibular depression), results in drastically reduced gape. Small gape during protrusion allows for the manipulation of water flow within the oropharyngeal cavity.

When common carp feed in aquaria, the animals typically move in a straight path, while their mouths (and to a lesser extent, their heads as a whole) rotate slightly from side to side. This allows the animal to forage on a wider area of substrate without necessitating whole-body movement, though it still necessitates modulation of the specific direction in which the mouth is facing. We classify this source of variation as flexibility, as the animal is responding to variation in stimuli by pointing its mouth in different directions. This flexibility should not be confused with the flexibility to perform open and closed mouth behaviors. In the former, the animal is performing an open mouth protrusion, but performing it in a slightly different direction in response to food position. Similar flexibility is also seen in cyprinodontiform fishes, which alter their jaw protrusion kinematics in response to specific prey location (Ferry-Graham et al., 2008). Such flexibility suggests a great ability to modulate feeding kinematics within both lineages (Wainwright et al., 2008).

Stereotypy: food gathering is more variable than food processing

Open mouth protrusions are less stereotyped (show more between-trial variability) (*sensu* Wainwright et al., 2008) than closed mouth protrusions. This observed difference in stereotypy may be actively controlled by the animal, *via* a behavioral 'decision' to conduct open

mouth protrusions in a variety of ways, or there may be passive mechanisms governing stereotypy; given their configuration in a closed mouth protrusion, the bones are mechanically constrained to move in a particular way. Open mouth protrusions are used in food gathering, where an organism needs to interact with its environment and to 'point' its suction flow in the appropriate direction to gather food. Increases in stereotypy observed during closed mouth protrusions could, on one hand, be explained by the fact that the animal is largely concerned with flushing water around inside the buccal cavity. On the other hand, the necessity of keeping the lips closely apposed during closed mouth protrusions causes mechanical coupling between the premaxillae and mandible that could increase stereotypy through mechanical constraint.

Flexibility with coordination: jaw (de)coupling

At the level of open *versus* closed mouth protrusions, the protrusion mechanism is inflexible, as shown by the magnitudes of kinethmoid rotation (KIN_{rz}) and bridge translation (BR_{tz}). However, other movements such as rotation of the maxilla (MX_{rz}) and jaw depression (MND_{rz}) do show flexibility in this realm (Fig. 6). The inflexibility of the protrusion mechanism combined with the high degree of coordination between KIN_{rz} and protrusion indicates that protrusion maintains a robust mechanism that is at least partially decoupled from lower jaw depression. Despite indications of decoupling, MND_{rz} still shows high coordination with kinethmoid rotation, even in closed mouth protrusions. This coordination could indicate that the lower jaw needs to be moving for the protrusion mechanism to function. Initial posture may also contribute to the protrusion mechanism (Ballintijn et al., 1972). The data we have presented herein suggest that these aspects of mandible posture and dynamics could be important to premaxillary protrusion in common carp.

This decoupling is potentially highly advantageous for the common carp, which sucks up matter from the substrate and sorts (winnows) food from non-food items. The animal can use one behavior for food acquisition (open mouth protrusions) and another for food sorting (closed mouth protrusions), with the two behaviors relying on the same underlying mechanism of premaxillary protrusion. This behavioral flexibility facilitates different functions of premaxillary protrusion when the mouth is open *versus* when it is closed. During open mouth protrusions, the function of premaxillary protrusion is: (1) to move the effective mouth position closer to the food without moving the whole body, (2) to increase the effective volume of the buccal cavity, and (3) to orient the suction flow in a particular direction. During closed mouth protrusions, the main function of premaxillary protrusion is to move buccal fluid either anteriorly (during protrusion) or posteriorly (during retraction). Carp are able to sort out food from detritus by pinning down the food particles that they intend to consume with the aid of the muscular palatal organ, flushing water back and forth through the oropharynx with the mouth closed, and subsequently expelling (either through the mouth or through the gill opening) non-food particles, leaving only the food in the buccal cavity for consumption (Sibbing and Uribe, 1985; Sibbing, 1988).

Closed mouth premaxillary protrusion during winnowing in surfperches (Embiotocidae) (Drucker and Jensen, 1991) is externally similar to closed mouth protrusion in carp. Surfperches use suspensorial abduction to decouple upper jaw protrusion from lower jaw depression, as opposed to the use of maxillary ventral translation by common carp. Despite differences in which linkage causes protrusion, both lineages have decoupled protrusion from lower jaw depression. Having evolved a secondary mechanism of premaxillary protrusion, both these lineages have broken a constructional constraint, and thereby expanded their functional repertoire. Without the constraint of coupling between those movements, both lineages are free to sort food from non-food by using closed mouth protrusions to force water anteriorly.

Our conclusions above may not accurately describe protrusion mechanics in all cypriniform taxa. Not all cypriniforms have the A1β muscle, and the diversity in shape of the kinethmoid among these taxa is impressive (Hernandez et al., 2007). Cypriniforms also exhibit a huge diversity of trophic niches (Simons and Gidmark, 2010) (Gidmark and Simons, in press); detritivory, herbivory, molluscivory, planktivory and piscivory are all represented within this order. Some of these trophic guilds employ large premaxillary protrusions and some do not.

Concluding remarks

We have shown that the functional significance of premaxillary protrusion in the carp is not limited to prey capture. This study has contributed to our understanding of kinethmoid-mediated premaxillary protrusion in five specific ways: (1) by exploring 3D bone movements using explicit, anatomically based coordinate systems, we have provided a framework for future comparison between species and proposed hypotheses for mechanically important connections between bones; (2) using an analysis of coordination, we have developed two alternative hypotheses for protrusion mechanics; (3) by examining the flexibility of different aspects of the mechanical system, we have refined our mechanical hypotheses and underscored the importance of examining bone posture as a defining aspect of biomechanical modeling; (4) by investigating the stereotypy in skeletal movements, we have linked the mechanics of jaw protrusion with the ecological function that these behaviors play in the natural environment; (5) by comparing our flexibility and coordination results with results from other species, we have demonstrated evolutionary parallels in control and decoupling in jaw mechanics. The diversity of kinethmoid shape among cypriniform taxa is substantial (Hernandez et al., 2007), and future studies using our techniques and other approaches will likely lead to diverse mechanical models and functional explorations of this peculiar bone. We hope that this mechanical description of a generalized omnivorous scum sucker with a relatively simple kinethmoid morphology is the first step towards understanding the mechanics, functional morphology and evolution of this bone.

ACKNOWLEDGEMENTS

We thank the Brown University morphology group and the members of the XROMM collaboration for insightful discussions, technology development and support throughout this study, as well as their criticisms of this manuscript. Specifically, we thank Ariel Camp, Kevin Conway, Angela Horner, Nicolai Konow, Bryan Nowroozi and Andrew Simons for their insights. David Baier, Stephen Gatesy, Edward Mullen, Daniel Riskin and Charles Vickers Jr provided pivotal expertise and advice on experimental design, implementation and analysis. Carly Lochala helped with laser scanning.

FUNDING

Funding was provided by the Bushnell Graduate Education and Research Fund, the W. M. Keck Foundation, a Grant-in-Aid-of-Research from the George Washington Chapter of Sigma Xi to K.L.S., and the National Science Foundation [grants DBI-0552051, IOS-0840950 and IOS-1120967 to E.L.B.; and grants IOS-0615827 and IOS-102548 to L.P.H.].

REFERENCES

Alexander, R. McN. (1966). The functions and mechanisms of the protrusible upper jaws of two species of cyprinid fish. *J. Zool.* **149**, 288-296.

Ballintijn, C. M., van den Burg, A. and Egberink, B. P. (1972). An electromyographic study of the adductor mandibulae complex of a free-swimming carp (*Cyprinus carpio L.*) during feeding. *J. Exp. Biol.* **57**, 261-283.

Benjamin, M. (1989). Hyaline-cell cartilage (chondroid) in the heads of teleosts. *Anat. Embryol.* **179**, 285-303.
Brainerd, E. L., Baier, D. B., Gatesy, S. M., Hedrick, T. L., Metzger, K. A., Gilbert, S. L. and Crisco, J. J. (2010). X-ray reconstruction of moving morphology (XROMM): precision, accuracy and applications in comparative biomechanics research. *J. Exp. Zool.* **313A**, 262-279.
Britz, R., Conway, K. W. and Ruber, L. (2009). Spectacular morphological novelty in a miniature cyprinid fish, *Danionella dracula* n. sp. *Proc. R. Soc. B.* **276**, 2179-2186.
Callan, W. T. and Sanderson, S. L. (2003). Feeding mechanisms in carp: crossflow filtration, palatal protrusions and flow reversals. *J. Exp. Biol.* **206**, 883-892.
Conway, K. W., Hirt, V. M., Yang, L., Mayden, R. L. and Simons, A. M. (2010). Cypriniformes: systematics and paleontology. In *Origin and Phylogenetic Interrelationships of Teleosts* (ed. J. S. Nelson, H. P. Schultze and M. V. H. Wilson), pp. 295-316. München, Germany: Verlag Dr Friedrich Pfeil.
Danos, N. and Staab, K. L. (2010). Can mechanical forces be responsible for novel bone development and evolution in fishes? *J. Appl. Ichthyol.* **26**, 156-161.
Dawson, M. M., Metzger, K. A., Baier, D. B. and Brainerd, E. L. (2011). Kinematics of the quadrate bone during feeding in mallard ducks. *J. Exp. Biol.* **214**, 2036-2046.
Drucker, E. G. and Jensen, J. S. (1991). Functional analysis of a specialized prey processing behavior: winnowing by surfperches (Teleostei: Embiotocidae). *J. Morphol.* **210**, 267-287.
Eaton, T. H., Jr (1935). Evolution of the upper jaw mechanism in Teleost fishes. *J. Morphol.* **58**, 157-172.
Ferry-Graham, L. A., Gibb, A. C., Hernandez, L. P. (2008). Premaxillary movements in cyprinodontiform fishes: an unusual protrusion mechanism facilitates 'picking' prey capture. *Zool.* **111**, 455-466.
Gatesy, S. M., Baier, D. B., Jenkins, F. A. and Dial, K. P. (2010). Scientific rotoscoping: a morphology-based method of 3-D motion analysis and visualization. *J. Exp. Zool.* **313A**, 244-261.
German, R., Campbell-Malone, R., Crompton, A., Ding, P., Holman. S., Konow, N. and Thexton, A. (2011). The concept of hyoid posture. *Dysphagia* **26**, 97-98.
Gidmark, N. J. and Simons, A. M. (in press). Cyprinidae: minnows and carps. In *North American Freshwater Fishes: Natural History, Ecology, and Conservation* (ed. M. L. Warren and B. Burr). Baltimore: Johns Hopkins Press.
Giris, S. (1952). The bucco-pharyngeal feeding mechanism in an herbivorous bottom-feeding cyprinoid, *Labeo horie* (Cuvier). *J. Morphol.* **90**, 281-315.
Grood, E. S. and Suntay, W. J. (1983). A joint coordinate system for the clinical description of 3-dimensional motions – application to the knee. *J. Biomech. Eng.* **105**, 136-144.
Hernandez, L. P., Bird, N. C. and Staab, K. L. (2007). Using zebrafish to investigate cypriniform evolutionary novelties: functional development and evolutionary diversification of the kinethmoid. *J. Exp. Zool. B* **308**, 625-641.
Motta, P. J. (1984). Mechanics and functions of jaw protrusion in teleost fishes: a review. *Copeia* **1984**, 1-18.
Osse, J. W., Sibbing, F. A. and Van den Boogaart, J. G. M. (1997). Intra-oral food manipulation of carp and other cyprinids: adaptations and limitations. *Acta. Physiol. Scand.* **161 Suppl.**, 47-57.
Sibbing, F. A. (1982). Pharyngeal mastication and food transport in the carp (*Cyprinus carpio L.*): a cineradiographic and electromyographic study. *J. Morphol.* **172**, 223-258.
Sibbing, F. A. (1985). Food processing in the orobranchial cavity of the carp. In *Fortschritte der Zoologie, Band 30* (ed. G. Fleischer and H. R. Duncker). Stuttgart: Gustav Fischer Verlag.
Sibbing, F. A. (1988). Specializations and limitations in the utilization of food resources by the common carp, *Cyprinus carpio:* a study of oral food processing. *Environ. Biol. Fish.* **22**, 161-178.
Sibbing, F. A. (1989). How do cyprinid fish select food from waste in their mouth? In *Progress in Zoology*, Vol. 35, *Trends in Vertebrate Morphology* (ed. H. Splechtna and H. Hilgers), pp. 519-520. Stuttgart: Gustav Fischer Verlag.
Sibbing, F. A. and Uribe, R. (1985). Regional specializations in the oro-pharyngeal wall and food processing in the carp (*Cyprinus carpio L.*). *Neth. J. Zool.* **35**, 377-422.
Simons, A. M. and Gidmark, N. J. (2010). Systematics and phylogenetic relationships of Cypriniformes. In *Gonorynchiformes and Ostariophysan Relationships: A Comprehensive Review* (ed. T. Grande). Enfield, NH, USA: Science Publishers Press.
Staab, K. L. and Hernandez, L. P. (2010). Development of the Cypriniform protrusible jaw complex in *Danio rerio*: constructional insights for evolution. *J. Morphol.* **271**, 814-825.
Staab, K. L., Ferry, L. A. and Hernandez, L. P. (2012). Comparative kinematics of cypriniform premaxillary protrusion. *Zoology* **115**, 65-77.
Tashman, S. and Anderst, W. J. (2003). *In-vivo* measurement of dynamic joint motion using high speed biplane radiography and CT: application to canine ACL deficiency. *J. Biomech. Eng.* **125**, 238-245.
Wainwright, P. C., Mehta, R. S. and Higham, T. E. (2008). Stereotypy, flexibility, and coordination: key concepts in behavioral functional morphology. *J. Exp. Biol.* **211**, 3523-3528.